An in vitro model to evaluate the impact of environmental fine particles (PM0.3-2.5) on skin damage

Anthony Verdin, Fabrice Cazier, Richard Fitoussi, Natacha Blanchet, Katell Vié, Dominique Courcot, Isabelle Momas, Nathalie Seta, Sophie Achard

An *in vitro* model to evaluate the impact of environmental fine particles ($PM_{0.3-2.5}$) on skin damages

Anthony Verdin[a], Fabrice Cazier[b], Richard Fitoussi[c], Natacha Blanchet[c], Katell Vié[c], Dominique Courcot[a,b], Isabelle Momas[d], Nathalie Seta[d,e] Sophie Achard[d,*]

[a] Unité de Chimie Environnementale et Interactions sur le Vivant EA4492, SFR Condorcet FR CNRS 3417, Université du Littoral Côte d'Opale, 59140 Dunkerque, France

[b] Centre Commun de Mesures (CCM), Université du Littoral Côte d'Opale, 59140 Dunkerque, France

[c] Laboratoires Clarins, 95300 Pontoise, France

[d] "INSERM UMR 1153 - CRESS, HERA (Health Environmental Risk Assessment) research unit. Paris Descartes-Sorbonne Paris Cité University, Paris, France."

[e] AP-HP Hôpital Bichat, Laboratoire de Biochimie, 75018 Paris, France

***Corresponding author**

Sophie Achard

"INSERM UMR 1153 – CRESS, HERA (Health Environmental Risk Assessment) research unit. Paris Descartes-Sorbonne Paris Cité University, Faculty of Pharmacy of Paris, France.

Phone +33 153.739.730

Fax +33 143.253.876

sophie.achard@parisdescartes.fr

e-mail address

anthony.verdin@univ-littoral.fr

fabrice.cazier@univ-littoral.fr

natacha.blanchet@clarins.com

richard.fitoussi@clarins.com

katell.vie@clarins.com

dominique.courcot@univ-littoral.fr

isabelle.momas@parisdescartes.fr

nathalie.seta@parisdescartes.fr

sophie.achard@parisdescartes.fr

Abstract

Exposure to airborne particulate matter (PM) has significant effects on human health mainly leading to cardio-respiratory diseases. However very few data are available regarding the impact of PM on the skin, so to better understand the impact of fine particle ($PM_{0.3-2.5}$) on both inflammatory response and epidermal structure, we exposed a reconstructed human epidermis (RHE) to several doses of PM collected in Cotonou (Benin, West Africa). After 24h of exposure, inflammatory response, histological observations, and gene expression related to oxidative stress, antioxidant defense and structural damages were determined. No PM-linked changes in tissue morphology or membrane integrity were observable. PM was however cytotoxic in a dose dependent manner. An inflammatory response appeared as shown by the increase in IL-1α and IL-8 cytokine productions. PM also induced oxidative stress, leading to an increase in 4-HNE immunostaining and to the up-regulation of *HMOX1*, *MT1G* and *MT1E*. Finally, PM had a negative impact on fundamental skin functions such as tissue anchorage, cell differentiation, cornification / skin desquamation and apoptosis. Our data show that airborne fine particles have an adverse effect on skin integrity, most probably leading to accelerated ageing.

Keywords

Airborne fine particles; *In vitro* skin model; Inflammatory response; Oxidative stress; Premature skin ageing

Abbreviations

4-HNE: 4-hydroxynonenal, BSA: bovine serum albumin, DAPI: 4',6-diamidino-2-phenylindole dihydrochloride, PM: particulate matter, H&E: haematoxylin and eosin, MMP: metalloproteinase, PBS: phosphate buffered saline, RHE: Reconstructed Human Epidermis, RT-qPCR: real-time quantitative PCR

Acknowledgements

The authors would like to thank Dr Marie-Odile FAURE, Scientific Consulting For You and Dr Philippe Crouzet, Estium-Concept, for scientific writing services on behalf of Clarins. They also wish to thank the Cellular and Molecular Imaging Platform, and Emeline Seurat from University Paris Descartes for technical supports and Gallic Beauchef from Clarins for useful comments and discussion.

1. Introduction

Air pollution is a degradation of air quality by introduction of harmful substances including gases, chemicals, biological contaminants, and particles. Air pollutants include particulate matter (PM), and are a major public health concern. PM is a heterogeneous and complex mixture due to its various origins (natural: soil, forest fires or volcanoes, and anthropogenic: human activities, industry, traffic…). Emitting sources and atmospheric conditions are key parameters contributing to the chemical and physical properties of ambient particulate matter (Kim et al., 2016). The role of the aerodynamic diameter of PM in the increase in the risks of chronic illness and premature death is widely documented. Much less recognized however, is that the chemical constituents adsorbed on PM also have significant effects on various diseases (Dergham et al., 2015; Kim et al., 2016; Song et al., 2013). A large number of studies have considered the effects of fine particles ($PM_{2.5}$) on human health, the majority being focused on respiratory and cardiovascular diseases. In the case of airway epithelium, for instance, the skin is in direct contact with airborne PM, and long-term exposure to PM may induce or exacerbate pre-existing skin diseases such atopic dermatitis,

acne, psoriasis, or premature skin ageing (Mancebo and Wang, 2015; Drakaki et al., 2014; Flohr and Mann, 2014; Kim et al., 2016). Different clinical studies have highlighted an increased level of rash after exposure to polluted air, a relation between traffic-associated pollution and eczema in children, a modification of the skin integrity, and a contribution of traffic-based air pollution to facial lentigines (Huls et al., 2016; Krutmann et al., 2014; Lefebvre et al., 2015; Vierkotter et al., 2010). At the cellular level, skin ageing modifies the tissue structure with looseness of the epidermal-dermal junction, and of the dermis with the reduction of blood vessels and nerves (Puizina-Ivic, 2008).

Oxidative stress seems to be one of the underlying mechanisms that induces adverse health effects and it is known to play a role in skin damage after exposure to some environmental factors like UV and pollutants (Carletto et al., 2000; Giacomoni and Rein, 2001; Krutmann et al., 2016; Lanuti and Kirsner, 2010; Makrantonaki et al., 2015; Valacchi et al., 2012). A direct impact of the UV exposure has been shown on vitamin D production, loss of elastic fiber properties, and oxidative stress (Gilchrest, 2013; Kammeyer and Luiten, 2015; Sherratt, 2013). Airborne pollutants such as nitrogen oxides, hydrocarbons, fine particles and ozone, also have a deleterious impact on skin, particularly sensitized skins which react more strongly to stressors (Krutmann et al., 2014). Similarly, some studies have established a link between tobacco smoke and skin alteration (Lecas et al., 2016; Morita et al., 2009; Urbanska et al., 2012a; Urbanska et al., 2012b).

Generation of reactive oxygen species, upregulation of pro-inflammatory factors by the arylhydrocarbon receptor (AhR), and keratinocytic VEGF up-regulation have been demonstrated as responsible mechanisms in the genesis of certain cutaneous pathologies (Bae et al., 2015; Krutmann et al., 2014; Li et al., 2003; Vierkotter and Krutmann, 2012). In order to better explain the underlying mechanisms, studies have been mainly performed on animals. A 6h exposure to controlled $PM_{2.5}$ was shown to induce oxidative stress (*HMOX1* expression)

in neonatal and adult rat lungs and the stimulation of antioxidant enzymes (*SOD1* for example) was observed for adults but not neonates, more susceptible to ultrafine particles (Chan et al., 2013). Cytotoxicity and apoptosis of human keratinocytes were also associated with combustion-generated organic nanoparticles (Pedata et al., 2012).

Mastrofrancesco et al. (2014) also reported that environmental pollution from diesel exhaust plays a critical role in the development of some autoimmune diseases (Mastrofrancesco et al., 2014). The authors showed that rat scleroderma skin keratinocytes and fibroblasts expressed cytokine genes (*IL-1α*, *IL-6*, *IL-8*, and *TNF-β*) at a higher level than control cells when treated with carbon-based nanoparticles collected from diesel exhaust. In addition, mRNA gene expressions of some *MMPs*, *Collagen types I* and *III*, and *VEGF* were significantly higher in untreated scleroderma skin cells than controls, with a dose dependent stimulation of all MMPs (Mastrofrancesco et al., 2014).

Taking into account that oxidative stress and inflammation play a major role in air pollution mediated toxicity of the skin, the aim of the present work was to evaluate the impact of environmental fine particles ($PM_{0.3\text{-}2.5}$), collected in a geographical area selected for its natural wealth in metallic elements, on skin tissue. For this purpose, we used a sensitive *in vitro* skin model (RHE) focusing on possible oxidative damage leading to morphological changes and modulation of protein expression.

2. Material and methods

2.1. Chemicals

Culture media, maintenance medium for experiment days, and growth medium for non-experiment days, were purchased from SkinEthic™, France. Penicillin-Streptomycin mixture (penicillin: 100 µg/mL; streptomycin: 100UI/mL) and Fungizon (Antibiotic-Antimycotic) were from Gibco (Invitrogen, WI, USA), Phosphate-buffered saline (PBS) from Biosolve Chimie (France), calcium chloride, goat serum, glycine, bovine serum albumin, glycerol,

sodium azide, Eukitt®, sodium cacodylate, glutaraldehyde, hexamethyldisilazane, osmium tetroxide, hydrochloric acid, and propylene oxide from Sigma-Aldrich (France). Acetic acid and Triton X100 were purchased from Merck (Germany); paraffin from Labonord (France); ethanol from VWR International (PA, USA). Xylene and paraformaldehyde (32%) were provided by Euromedex (France); sodium chloride by Minisol (France); Mayer Haematoxylin (RAL Diagnostics, France) and Eosin by Merck (Germany).

2.2. In vitro skin model

A reconstructed human epidermis from normal human keratinocytes provided the RHE model (SkinEthic™, France) (Rosdy and Clauss, 1990; Rosdy et al., 1993) that was used as described previously (Lecas et al., 2016). For all experiments, the same batch (MF22-5) was used. Signed informed consent and ethical approval were obtained by the supplier.

Upon reception RHEs were placed in an incubator at 37 °C, 5% CO_2 and 90% relative humidity. Experiments were carried out 24h after RHE-acclimation (Poumay et al., 2004).

2.3. Fine particles exposure ($PM_{0.3\text{-}2.5}$)

Detailed information about collection and physicochemical characteristics of the PM collected in Cotonou city (Benin, West Africa) have been previously published (Table 1, Table S1) (Cachon et al., 2014). After collection, $PM_{0.3\text{-}2.5}$ were weighed and stored at -20°C until experimentation. PM were suspended in the culture medium containing 1% fungizon and sonicated at 50W during 10 min (Bath sonicator Branson CPXH, Dutscher, France) to avoid the presence of aggregates (Fig. S1). RHEs were exposed to three PM concentrations: 3, 15 and 30 µg/cm^2 as published by Cachon (Cachon et al. 2014). 30 µL of suspension of the desired PM concentration were deposited directly on the apical surface of RHE tissues. RHEs were then placed on an orbital agitator for 10 mins to homogenize the PM suspension to the apical surface and then incubated at 37°C, 5% CO_2 in a humidified incubator.

After 24h exposure to PM, culture media were collected to assess biological activity: LDH release, cytokine and MMP quantifications. RHEs were harvested to perform MTT assay, histological / immunohistochemical analysis and mRNA quantification by RT-qPCR.

Two controls were used: medium-control (named Control: 30 µL of medium without PM deposited on apical surface) and incubator-control (without medium on apical side). As no difference was shown between these two controls, only the medium-control (Control) was introduced in the continuation of the present work.

2.4. Functional integrity

Colorimetric MTT [3-(4,5-dimethylthiazol-2-yl)-2,5-diphenyltetrazolium bromide] assay relies on the quantification of mitochondrial succinate dehydrogenase activity. Viable cells convert a soluble tetrazolium salt to a formazan product having a maximum photometric absorbance at a wavelength of 490 nm (Persoz et al., 2010). Absorbance was read with a microtiter plate reader (Multiskan-EX, Thermo Scientific). Experiments were repeated at least 4 times in duplicate.

2.5. Cellular viability: LDH release

Membrane integrity was determined by measuring the release of intracellular lactate dehydrogenase (LDH) into the basal culture medium (Lactacte deshydrogenase activity assay Kit, Sigma). LDH reduced NAD to NADH, which is detected by colorimetric at 450nm using a microtiter plate reader (Multiskan-EX, Thermo Scientific). LDH release is the reflection of the cellular viability and was expressed as an arbitrary unit. Experiments were repeated at least 4 times in duplicate.

2.6. Proinflammatory mediator quantification

Two cytokines, interleukin 1α (IL-1α #KAC1191) and interleukin 8 (IL-8 #KHC0081), were assessed using an ELISA assay following manufacturer's instructions (Novex™, France). Optical densities were determined using a microplate-reader (Multiskan-EX, Thermo

Scientific, USA) set to 450 nm. Calibration curves were established using Ascent Software® (Thermo Scientific, MA, USA). Cytokine concentrations were expressed in pg/mL. The limits of quantification were 3.9 and 15.6 pg/mL for IL-1α and IL-8 respectively. Experiments were repeated 4 times in duplicate.

2.7. Matrix metalloproteinases assessment

Assessment of matrix metalloproteinases was performed using a multiplex panel (Human Magnetic Luminex Performance Assay Base Kit, MMP Panel [#LMPM000] R&D Systems, France). Samples were incubated overnight with antibody-coated beads at 4°C under constant shaking. The following day, plates were washed twice and secondary antibody was added to the samples for one-hour incubation at room temperature under constant shaking. Then, plates were incubated for 30 minutes with streptavidin labelled with R-Phycoerythrin at room temperature under agitation. Washing process was repeated, before adding sheath fluid and reading the results using Luminex® technology (Magpix®, Bio-Rad, France) after 5 minutes shaking. Concentrations were calculated out of standard curves using recombinant proteins and expressed in pg/mL. Experiments were repeated 2 times in triplicate.

2.8. Histological and immunochemical assessments

Histological and immunohistochemical assessments were performed 24h after exposure. RHEs were fixed in 4% paraformaldehyde for 4h and paraffin-embedded sections were sliced for Mayer Haematoxylin and Eosin (H&E) and for immunohistochemistry.

Prior to Mayer H&E staining, RHE cross-sections (4 µm) went through xylene deparaffinization and rehydration with graded ethanol baths. Observations were made with an inverted light microscope (Leica DM4000 B LED).

For immunohistochemistry, sections were blocked in 10% BSA/PBS before incubation with anti-loricrin or anti-4-HNE primary antibodies (#ab24722 and #ab46545 respectively, Abcam, UK). For both, an AlexaFluor®488-conjugated goat anti-mouse (#A-21121,

Invitrogen, USA) was used as a secondary antibody. Nuclei were stained with 4',6-diamidino-2-phenylindole dihydrochloride (DAPI, #32670 Sigma, France). The resulting immunofluorescence was observed under a Nikon Eclipse 50i fluorescence microscope and pictures were taken using Nikon NIS Elements software. Quantification of both loricrin and 4-HNE fluorescence signals of tissue sections was performed using Visilog software version 7.0. Experiments were repeated in 3 independent experiments.

2.9. RNA isolation and RT-qPCR

Following the manufacturer's instructions, total RNA was extracted from tissues using the RNeasy® miniKit (Qiagen, Germany). RNA quality and quantity were checked with the 2100-Bioanalyzer (Agilent Technologies, France), then RNA was reverse transcribed using the Transcriptor Universal cDNA Master (Roche Diagnostics, Switzerland). PCR primers were designed according to the Roche Universal Probe Library Assay Design Center (www.universalprobelibrary.com). A LightCycler 480 system using LightCycler 480 Probes Master (Roche, Germany) was used to perform quantitative RT-qPCR on 29-gene epidermal function plates (Agilent RNA Nano chips #5067-1511, Roche Diagnostics, Switzerland). The $2^{-\Delta\Delta Ct}$ method provided N-fold differential expression of mRNA gene expression and results were obtained by calculating the fold change (FC) between two conditions, exposed *versus* control, meaning the expression difference. mRNA expression was considered as increased when FC $\geq$ 1.5, while decreased when FC $\leq$ 0.7. GAPDH and RPL13 housekeeping genes were used as internal controls. Results are the mean of one experiment assessed in duplicate.

2.10. Statistical analysis

Data are displayed as mean ± standard deviation. All experiments were repeated at least in duplicate in two different experiments; the number of experiments conducted is indicated in the legend of each Figure. Results were analyzed by one-way ANOVA followed by a

Tukey-Kramer post-test. Statistical analysis was performed using JMP v.10 (SAS division, USA). $p < 0.05$ was considered significant.

3. Results

3.1. Tissue morphology and cell functionality (Fig. 1-2)

The SkinEthic reconstituted human epidermis (RHE) model consists of the four characteristic layers *stratum germinativum*, *stratum spinosum*, *stratum granulosum*, and *stratum corneum* as shown in the Figure 1A.

A 24h exposure of RHEs to increasing PM concentrations (3, 15 and 30 µg/cm^2) did not induce structural changes whatever the PM-level tested (Figs. 1B1, 1B2, 1B3): RHEs exposed to PM were similar to the Control. This observation is confirmed by the absence of LDH release certifying good membrane integrity (Fig. 2B). Nevertheless, MTT assay revealed a dose-dependent relation between the level of PM and cellular functionality, with a statistically significant decrease after exposure of RHEs at 15 and 30 µg/cm^2 compared to Control (Fig. 2A). This last result would seem to indicate that the mitochondrial succinate dehydrogenase function is disturbed without leading to cell death as indicated by LDH and morphology data.

3.2. Inflammatory response (Fig. 3)

To evaluate the inflammatory response of RHEs, the production of two cytokines, IL-1α and IL-8, was evaluated after RHE-exposure to PM at 3, 15 and 30 µg/cm^2. Compared to Control, a 24h-exposure to PM at 3 µg/cm^2 did not induce significant difference in the production levels of IL-1α and IL-8 (Fig. 3). For higher doses of PM (15 and 30 µg/cm^2), a significant dose-dependent increase in the production of the two cytokines tested was observed. For IL-8, the increase was as high as 52-fold the level detected in the Control after exposure of RHEs to 30 µg/cm^2 of PM.

Remark: These initial results concerning membrane integrity, functionality and inflammatory responses, revealed significant cytokine production after RHE exposure at the highest dose of

PM (30 µg/cm^2) without membrane integrity disorder (LDH release) but with a loss of 50% of cellular functionality, probably due to the oxidative stress caused by metallic compounds adsorbed on the PM tested. In this context, the rest of the study has been focused on the exposure of RHE tissue to PM at 30 µg/cm^2.

3.3. Oxidative stress (Fig. 4)

Two steps have been taken to assess oxidative damage on RHE tissue: 4-HNE immunostaining with quantification (4-hydroxynonenal, one of the most important products of lipid peroxidation) and three oxidant gene expressions evaluated by RT-qPCR.

Immunostaining of 4-HNE, a widely used marker of oxidative stress, showed a substantial increase in labelling, 24h after exposure of RHE tissue to PM at 30 µg/cm^2, compared to Control (Fig. 4A). The quantification of 4-HNE staining confirmed this significant increase by 4-fold, demonstrating that PM exposure does stimulate oxidative stress in our model (Fig. 4B). To investigate the underlying effects on the molecular and biological activities of RHE, the activity of three genes involved in oxidative stress (*HMOX1*, *MT1G* and *MT1E*) was studied by quantification of their mRNA. mRNA expression levels of the genes were stimulated by 1.6 to 3.0-fold respectively after exposure of RHEs to PM at 30 µg/cm^2 (Fig. 4C).

3.4. Differentiation and morphology (Fig. 5-6)

To evaluate the impact of PM on both extracellular matrix and tissue differentiation, two approaches were considered: MMP level quantification and loricrin immunostaining with quantification.

Immuno-quantification of matrix metalloproteinases panel showed that only two MMPs from the nine MMPs tested (MMP-1, -2, -3, -7, -8, -9, -10, -12, -13) were significantly modulated. Compared to Control, MMP-1 was induced by 1.5-fold and MMP-3 by 1.9-fold after exposure of RHEs to 30 µg/cm^2 of PM (Fig. 5). In addition, immunostaining of loricrin,

a major protein component of terminally differentiated epidermal cells, showed a significant decrease in labelling after PM-exposure (Fig. 6A). This result is confirmed by the quantification of the intensity of loricrin labelling. Compared to the Control, a 1.9-fold loss of loricrin staining was observed 24h after PM-exposure (Fig. 6B).

3.5. Other biological impacts of PM on RHEs (Fig. 7)

To investigate the underlying effects of PM at 30 µg/cm^2 on the biological activity of RHEs, 12 genes were selected as the most representative to evaluate cellular and molecular modulation. Differentiation genes were either weakly stimulated (*IVL*) or weakly decreased (*KRT1, KRT10*) (Fig. 7). Expressions of cell-cell junction genes (*EVPL* (*ENVOPLAKIN*), *GJA1*, *CDH1*, *CD44*), and anchorage genes (*COL7A1*, *COL4A1*) were suppressed after PM-exposure. Apoptotic gene expression was also studied (*CASP3*, *CDKN2A*, *BIRC5*), and results shown that upon PM exposure, *BIRC5* expression was reduced while *CDKN2A* expression was doubled and *CASP3* was highly stimulated (6.3-fold) (Fig. 7).

4. Discussion

The aim of our study was to better understand the impact of airborne fine particles (PM) on skin damage as suggested by other studies (Valacchi et al., 2012; Vierkotter and Krutmann, 2012).

In this study we used particles collected in Cotonou, an urban city of West Africa (Benin). Our objective was to generally test environmental particles rich in such metallic inorganic elements as metals, positively correlated with intracellular ROS production (Dergham et al., 2015), and not to specifically test Cotonou's PM. Having said this, the interest of particle samples tested in our study does lie in their origin: in African countries like Cotonou the soils are rich in iron oxide (Fe_2O_3) and aluminium oxide (Al_2O_3) (Kikouama et al., 2009), with co-existing heavy metals at very high levels (Alford et al., 2010; Cheng, 2003). In comparison we can note that the level of metallic elements in PM collected in an

298 urban city of France (Dunkerque) was 620 ng/m^3 *versus* 8,644 ng/m^3 in Cotonou (Dergham et
299 al., 2015).

300 The presence of such elements contributes to atmospheric pollution leading to various
301 biological dysregulations in Human, such as oxidative stress, this latter being at the origin of
302 various pathologies (Cachon et al., 2014). The choice of the *in vitro* skin model was important
303 to our study. RHE tissue consists of an epidermis without dermis, obtained from keratinocytes
304 cultured at high cell density on a polycarbonate filter membrane with 0.4 µm pore diameter.
305 After 15 days of culture, keratinocytes formed a differentiated epidermis with histological
306 features similar to those observed *in vivo*: a basal layer, spinous layer, granular layer, and a
307 stratum corneum (Poumay et al, 2004). This model was used to assess the irritating and/or
308 corrosive properties of some chemical compounds (Kandárová et al, 2006). However, like all
309 *in vitro* models, RHE tissue has some limitations, principally the small experimentation
310 window (3 days) due to the model ageing quickly (Lecas et al, 2016). This led us to limit our
311 experiments to 24h of exposure. Nevertheless, the RHE model did allow the combined
312 implementation of 3D-reconstituted tissue and exposure at the air-liquid interface in a
313 controlled environment. Our work has thus highlighted the possibility of using this *in vitro*
314 3D-skin model to assess the importance of the chemical constituents of PM on the cellular
315 and molecular responses of exposed tissue.

316 Exposure to airborne particulate matter has toxic effects on human health as illustrated by
317 drastic respiratory and skin diseases (Beelen et al., 2014; Drakaki et al., 2014; Raaschou-
318 Nielsen et al., 2013). The skin can be impacted by several intrinsic and extrinsic phenomena
319 (Makrantonaki et al., 2015). External factors such as UV and air pollutants including tobacco
320 smoke can play an important role in skin ageing (Valacchi et al., 2012; Vierkotter and
321 Krutmann, 2012). In order to take into account all levels (tissue, cell and molecular level) and
322 have a better knowledge on the underlying mechanisms, an *in vitro* RHE skin model can be

used to evaluate the toxicity level of extrinsic exposure such as tobacco smoke (Lecas et al., 2016) and airborne pollutants (Magnani et al., 2016). The mode of action (MoA) hypothesis of the impact of airborne pollution on the premature skin ageing process, using the RHE 3D-skin model exposed to fine particles, is illustrated in Figure 8.

While the PM did not induce obvious structural changes in RHE morphology and a loss of membrane integrity, it did lead to a dose-dependent decrease in cellular functionality as shown by MTT assay, evaluating mitochondrial succinate dehydrogenase activity, a mitochondrial enzyme. These results - showing a loss of cellular functionality with absence of both structural changes and tissue integrity injury - would appear contradictory, but is not. Specifically, the complementary nature of the tests gives a more accurate view of the impact of a xenobiotic on a targeted tissue. The oxidizing potential of PM, due to the presence of metal elements adsorbed on their surface, could explain this result and constitute the key event 1 (KE1, Fig. 8).

To consolidate this result, we observed that PM was able to stimulate IL-1α and IL-8 production in a dose dependent manner, thus illustrating the inflammatory response of skin tissue (AE1, Fig. 8). Oxidative stress was also induced, as illustrated by the increase of 4-HNE labelling in RHE (KE2, Fig. 8), and in accordance with the stimulation of *HMOX1* expression. A similar induction of *HMOX1*, a sensitive marker for oxidative stress, was observed upon exposure of a lung model to ultrafine particles (Chan et al., 2013; Li et al., 2003). In reaction, the tissue induces antioxidants as illustrated by previous works on the lung (Curjuric et al., 2012; Huang et al., 2009) and, in our case, by the induction of *MT1G* and *MT1E* expressions which corresponding proteins are known to be involved in heavy metal binding (KE3, Fig. 8).

Considering tissue integrity, no morphological changes appeared after PM-exposure, and increased levels of MMP-1 and MMP-3 production suggest an accelerated degradation of the

extracellular matrix (KE5, Fig. 8). The level of loricrin, a keratinocyte specific protein, was also decreased (AE2, Fig. 8). Moreover, cell-cell junction, anchorage, and terminal differentiation genes, except *Involucrin* (*IVL*), were drastically down-regulated on PM-exposure (AE3, Fig. 8). *Involucrin* (*IVL*) is known to play an important role in cornified envelope development (Hanel et al., 2013). Inhibition of *IVL* was observed in several studies, including when the *in vitro* RHE skin model was exposed to tobacco smoke, illustrating the disorganization of skin barrier function (Lecas et al., 2016). However, stimulation of *IVL* was also found after exposure of HaCaT cells and atopic dermatitis to ambient $PM_{2.5}$ leading to the hypothesis that cell death is the primary cause of skin alteration rather than protein modification (Hirao et al., 2003; Li et al., 2017). *KRT1* and *KRT10* expressions were decreased, revealing the skin barrier dysfunction (Pan et al., 2015). This tissue slackening was also illustrated by the decrease in the expression of cell-cell junction (*EVPL*, *GJA1*, *CDH1* and *CD44*) and anchorage (*COL4A1* and *COL7A1*) genes. This is in line with the role of Gap Junctions Intercellular Communications and Tight Junctions in the epithelial lining, which modification might be implied in cancer development after PM_{10} inhalation (Nemmar et al., 2013).

In order to better understand the underlying mechanism of toxicity on the RHE model, apoptosis-linked genes (*CASP3*, *CDKN2A* and *BIRC5* (*SURVIVIN*)) were also investigated. *BIRC5*, known to block apoptosis and to regulate the cell cycle, was downregulated. Moreover, both *CASP3* and *CDKN2A*, pro-apoptotic genes, were upregulated in our study (6- and 2-fold, respectively) (KE4, Fig. 8). Metal elements, being the main components of PM from Cotonou, have been described as inductors of *CASP3* in hepatic cells and macrophages (Andreau et al., 2012). *CDKN2A* (p16) is known to have an ageing-dependent expression and therefore to be increased in the elderly (Ressler et al., 2006).

In conclusion, using an *in vitro* 3D-model of human reconstituted epidermis, our results showed that exposure to fine particles lead to an increase in some indicators such as oxidative stress and inflammatory response, contributing to a tissue slackening following the degradation of the extracellular matrix and cell-cell junctions. The chemical composition of airborne particulate matter, and more particularly the metallic elements adsorbed on the surface of the PM, could contribute to various MoA hypotheses leading to the premature skin ageing and the loss of the protective role of the cutaneous barrier. The present work is original and innovative, and provides new development opportunities to better understand the role of atmospheric particulate matter on skin damage.

Funding

This research did not receive any specific grant from funding agencies in the public, commercial, or not-for-profit sectors.

Competing interests

R. Fitoussi, N. Blanchet and K. Vié are full-time employees of Clarins, a major company specialized in the design, manufacturing and marketing of cosmetic products.

References

Alford, É. R., Pilon-Smits, E. A. H., Paschke, M. W., 2010. Metallophytes—a view from the rhizosphere. Plant and Soil 337, 33-50.

Andreau, K., Leroux, M., Bouharrour, A., 2012. Health and cellular impacts of air pollutants: from cytoprotection to cytotoxicity. Biochem. Res. Int. 2012, 493894.

Bae, O. N., Noh, M., Chun, Y. J., Jeong, T. C., 2015. Keratinocytic vascular endothelial growth factor as a novel biomarker for pathological skin condition. Biomol. Ther. 23, 12-18.

Beelen, R., Raaschou-Nielsen, O., Stafoggia, M., Andersen, Z.J., Weinmayr, G., Hoffmann, B., Wolf, K., Samoli, E., Fischer, P., Nieuwenhuijsen, M., Vineis, P., Xun, W.W., Katsouyanni, K., Dimakopoulou, K., Oudin, A., Forsberg, B., Modig, L., Havulinna, A.S., Lanki, T., Turunen, A., Oftedal, B., Nystad, W., Nafstad, P., De Faire, U., Pedersen, N.L., Ostenson, C.G., Fratiglioni, L., Penell, J., Korek, M., Pershagen, G., Eriksen, K.T., Overvad, K., Ellermann, T., Eeftens, M., Peeters, P.H., Meliefste, K., Wang, M., Bueno-de-Mesquita, B., Sugiri, D., Kramer, U., Heinrich, J., de Hoogh, K., Key, T., Peters, A., Hampel, R., Concin, H., Nagel, G., Ineichen, A., Schaffner, E., Probst-Hensch, N., Kunzli, N., Schindler, C., Schikowski, T., Adam, M., Phuleria, H., Vilier, A., Clavel-Chapelon, F., Declercq, C., Grioni, S., Krogh, V., Tsai, M.Y., Ricceri, F., Sacerdote C., Galassi, C., Migliore, E., Ranzi, A., Cesaroni, G., Badaloni, C., Forastiere, F., Tamayo, I., Amiano, P., Dorronsoro, M., Katsoulis, M., Trichopoulou, A., Brunekreef, B., Hoek, G., 2014. Effects of long-term exposure to air pollution on natural-cause mortality: an analysis of 22 European cohorts within the multicentre ESCAPE project. Lancet (London, England) 383, 785–795.

Cachon, B. F., Firmin, S., Verdin, A., Ayi-Fanou, L., Billet, S., Cazier, F., Martin, P. J., Aissi, F., Courcot, D., Sanni, A.,Pirouz S., 2014. Proinflammatory effects and oxidative stress within human bronchial epithelial cells exposed to atmospheric particulate matter (PM(2.5) and PM(>2.5)) collected from Cotonou, Benin. Environ. Pollut. (Barking, Essex : 1987) 185, 340-51.

Carletto, C., Nicolay, J. F., Courbebaisse, Y., 2000. Oxidative stress and cutaneous ageing: the 'toxic second messengers' concept and an interesting family of products, 'pseudodipeptides'. Int. J. Cosmetic Sci. 22, 361-370.

Chan, J. K., Charrier, J. G., Kodani, S. D., Vogel, C. F., Kado, S. Y., Anderson, D. S., Anastasio, C., Van Winkle, L. S., 2013. Combustion-derived flame generated ultrafine

soot generates reactive oxygen species and activates Nrf2 antioxidants differently in neonatal and adult rat lungs. Part. Fibre Toxicol. 10, 34.

Cheng, S., 2003. Heavy metal pollution in China: origin, pattern and control. Environ. Sci. Pollut. Res. Int. 10, 192-198.

Curjuric, I., Imboden, M., Nadif, R., Kumar, A., Schindler, C., Haun, M., Kronenberg, F., Kunzli, N., Phuleria, H., Postma, D. S., Russi, E.W., 2012. Different genes interact with particulate matter and tobacco smoke exposure in affecting lung function decline in the general population. PloS one 7, e40175.

Dergham, M., Lepers, C., Verdin, A., Cazier, F., Billet, S., Courcot, D., Shirali, P., Garcon, G., 2015. Temporal-spatial variations of the physicochemical characteristics of air pollution Particulate Matter (PM2.5-0.3) and toxicological effects in human bronchial epithelial cells (BEAS-2B). Environ. Res. 137, 256-267.

Drakaki, E., Dessinioti, C., Antoniou, C. V., 2014. Air pollution and the skin. Front. Environ. Sci. 2, 1-6.

Flohr, C., Mann, J., 2014. New insights into the epidemiology of childhood atopic dermatitis. Allergy 69, 3-16.

Giacomoni, P. U., Rein, G., 2001. Factors of skin ageing share common mechanisms. Biogerontology 2, 219-229.

Gilchrest, B. A., 2013. Photoaging. J. Invert. Dermatol. 133, E2-E6.

Hanel, K. H., Cornelissen, C., Luscher, B., Baron, J. M., 2013. Cytokines and the skin barrier. Int. J. Mol. Sci. 14, 6720-6745.

Hirao, T., Terui, T., Takeuchi, I., Kobayashi, H., Okada, M., Takahashi, M., Tagami, H., 2003. Ratio of immature cornified envelopes does not correlate with parakeratosis in inflammatory skin disorders. Exp. Dermatol. 12, 591-601.

Huang, Y. C., Li, Z., Carter, J. D., Soukup, J. M., Schwartz, D. A., Yang, I. V., 2009. Fine ambient particles induce oxidative stress and metal binding genes in human alveolar macrophages. Am. J. Respir. Cell. Mol. 41, 544-552.

Huls, A., Vierkotter, A., Gao, W., Kramer, U., Yang, Y., Ding, A., Stolz, S., Matsui, M., Kan, H., Wang, S., Jin, L., Krutmann, J., Schikowski, T., 2016. Traffic-Related Air Pollution Contributes to Development of Facial Lentigines: Further Epidemiological Evidence from Caucasians and Asians. J. Investig. Dermatol. 136, 1053-1056.

Kandárová, H., Liebsc, M., Spielmann, H., Genschow, E., Schmidt, E., Traue, D., Guest, R., Whittingham, A., Warren, N., Gamer, A. O., Remmele, M., Kaufmann, T., Wittmer, E., De Wever, B., Martin Rosdy M., 2006. Assessment of the human epidermis model SkinEthic RHE for in vitro skin corrosion testing of chemicals according to new OECD TG 431. Toxicol. In Vitro 2, 547–559.

Kammeyer, A., Luiten, R. M., 2015. Oxidation events and skin aging. Ageing Res. Rev. 21, 16-29.

Kikouama, J., Konan, K., Katty, A., Bonnet, J., Balde, L., Yagoubi, N., 2009. Physicochemical characterization of edible clays and release of trace elements. Appl. Clay Sci. 43, 135-141.

Kim, K. E., Cho, D., Park, H. J., 2016. Air pollution and skin diseases: Adverse effects of airborne particulate matter on various skin diseases. Life Sciences 152, 126-134.

Krutmann, J., Bouloc, A., Sore, G., Bernard, B. A., Passeron, T., 2017. The skin aging exposome. J. Dermatol. Sci. 85, 152-161.

Krutmann, J., Liu, W., Li, L., Pan, X., Crawford, M., Sore, G., Seite, S., 2014. Pollution and skin: from epidemiological and mechanistic studies to clinical implications. J. Dermatol. Sci. 76, 163-168.

Lanuti, E. L., Kirsner, R. S., 2010. Effects of pollution on skin aging. J. Investig. Dermatol. 130, 2696.

Lecas, S., Boursier, E., Fitoussi, R., Vie, K., Momas, I., Seta, N., Achard, S., 2016. In vitro model adapted to the study of skin ageing induced by air pollution. Toxicol. Lett. 259, 60-68.

Lefebvre, M. A., Pham, D. M., Boussouira, B., Bernard, D., Camus, C., Nguyen, Q. L., 2015. Evaluation of the impact of urban pollution on the quality of skin: a multicentre study in Mexico. Int. J. Cosmetic Sci. 37, 329-338.

Li, N., Sioutas, C., Cho, A., Schmitz, D., Misra, C., Sempf, J., Wang, M., Oberley, T., Froines, J., Nel, A., 2003. Ultrafine particulate pollutants induce oxidative stress and mitochondrial damage. Environ. Health Perspect. 111, 455-460.

Li, Q., Kang, Z., Jiang, S., Zhao, J., Yan, S., Xu, F., Xu, J., 2017. Effects of Ambient Fine Particles PM2.5 on Human HaCaT Cells. Int. J. Environ. Res. Public Health 14, 1-10.

Magnani, N. D., Muresan, X. M., Belmonte, G., Cervellati, F., Sticozzi, C., Pecorelli, A., Miracco, C., Marchini, T., Evelson, P., Valacchi, G., 2016. Skin Damage Mechanisms Related to Airborne Particulate Matter Exposure. Toxicol. Sci. 149, 227-236.

Makrantonaki, E., Vogel, M., Scharffetter-Kochanek, K., Zouboulis, C. C., 2015. [Skin aging: Molecular understanding of extrinsic and intrinsic processes]. Hautarzt 66, 730-737.

Mancebo, S. E., Wang, S. Q., 2015. Recognizing the impact of ambient air pollution on skin health. J. Eur. Acad. Dermatol. Venereo., JEADV 29, 2326-2332.

Mastrofrancesco, A., Alfe, M., Rosato, E., Gargiulo, V., Beatrice, C., Di Blasio, G., Zhang, B., Su, D. S., Picardo, M., Fiorito, S., 2014. Proinflammatory effects of diesel exhaust nanoparticles on scleroderma skin cells. J. Immunol. Res. 2014, 138751.

Morita, A., Torii, K., Maeda, A., Yamaguchi, Y., 2009. Molecular basis of tobacco smoke-induced premature skin aging. J. Investig. Dermatol. Symp. Proc. 14, 53-55.

494 Nemmar, A., Holme, J. A., Rosas, I., Schwarze, P. E., Alfaro-Moreno, E., 2013. Recent
495 advances in particulate matter and nanoparticle toxicology: a review of the in vivo and in
496 vitro studies. Biomed. Res. Int. 2013, 279371.
497 Pan, T. L., Wang, P. W., Aljuffali, I. A., Huang, C. T., Lee, C. W., Fang, J. Y., 2015. The
498 impact of urban particulate pollution on skin barrier function and the subsequent drug
499 absorption. J. Dermatol. Sci 78, 51-60.
500 Pedata, P., Boccellino, M., La Porta, R., Napolitano, M., Minutolo, P., Sgro, L. A., Zei, F.,
501 Sannolo, N., Quagliuolo, L., 2012. Interaction between combustion-generated organic
502 nanoparticles and biological systems: in vitro study of cell toxicity and apoptosis in
503 human keratinocytes. Nanotoxicology 6, 338-352.
504 Persoz, C., Achard, S., Leleu, C., Momas, I., Seta, N., 2010. An in vitro model to evaluate the
505 inflammatory response after gaseous formaldehyde exposure of lung epithelial cells.
506 Toxicol. Lett. 195, 99-105.
507 Poumay, Y., Dupont, F., Marcoux, S., Leclercq-Smekens, M., Herin, M., Coquette, A., 2004.
508 A simple reconstructed human epidermis: preparation of the culture model and utilization
509 in in vitro studies. Arch. Dermatol. Res. 296, 203-211.
510 Puizina-Ivic, N., 2008. Skin aging. Acta Dermatovenerol. Alp. Pannonica Adria. 17, 47-54.
511 Raaschou-Nielsen, O., Andersen, Z. J., Beelen, R., Samoli, E., Stafoggia, M., Weinmayr, G.,
512 Hoffmann, B., Fischer, P., Nieuwenhuijsen, M. J., Brunekreef, B., et al., 2013. Air
513 pollution and lung cancer incidence in 17 European cohorts: prospective analyses from
514 the European Study of Cohorts for Air Pollution Effects (ESCAPE). The Lancet.
515 Oncology 14, 813-822.
516 Ressler, S., Bartkova, J., Niederegger, H., Bartek, J., Scharffetter-Kochanek, K., Jansen-Dürr,
517 P., Wlaschek, M., 2006. p16 INK4A is a robust in vivo biomarker of cellular aging in
518 human skin. Aging Cell 5, 379-389.

519 Sherratt, M. J., 2013. Age-Related Tissue Stiffening: Cause and Effect. Adv. Wound Care 2,
520 11-17.
521 Song, S., Paek, D., Lee, K., Lee, Y. M., Lee, C., Park, C., Yu, S. D., 2011. Effects of ambient
522 fine particles on pulmonary function in children with mild atopic dermatitis. Arch.
523 Environ. Occup. Health. 68, 228-34.
524 Urbanska, M., Nowak, G., Florek, E., 2012a. Cigarette smoking and its influence on skin
525 aging. Przegl. Lek., 1111-1114.
526 Urbanska, M., Ratajczak, L., Witkowska-Nagiewicz, A., 2012b. [Analysis of knowledge
527 about tobacco smoking influence on skin condition]. Przegl. Lek., 69, 1055-1059.
528 Valacchi, G., Sticozzi, C., Pecorelli, A., Cervellati, F., Cervellati, C., Maioli, E., 2012.
529 Cutaneous responses to environmental stressors. Ann. N. Y. Acad. Sci. 1271, 75-81.
530 Vierkotter, A., Krutmann, J., 2012. Environmental influences on skin aging and ethnic-
531 specific manifestations. Dermatoendocrinol. 4, 227-231.
532 Vierkotter, A., Schikowski, T., Ranft, U., Sugiri, D., Matsui, M., Kramer, U., Krutmann, J.,
533 2010. Airborne particle exposure and extrinsic skin aging. J. Invest. Dermatol. 130, 2719-
534 2726.
535
536
537
538
539
540
541
542

Figure legends

Fig. 1. Morphological observations of RHEs after PM-exposure.

RHE tissues were exposed to PM at 0 (Control), 3, 15, or 30 µg/cm² for 24h. After exposure RHEs were fixed in 4% paraformaldehyde and cross-sections (4 µm) were stained with Mayer Haematoxylin and Eosin (H&E) and observed using an inverted light microscope (Leica DM4000B LED).

Scale bar represents 25 µm ; 40x magnification. Representative pictures of n=3 independent experiments.

(A) RHE Control. 1/*Stratum germinativum*; 2/*Stratum spinosum*; 3/*Stratum granulosum*; 4/*Stratum corneum*.

(B) RHE exposed at (B1) 3 µg/cm² ; (B2) 15 µg/cm² ; (B3) 30 µg/cm².

Fig. 2. Effects of PM on RHE functionality and membrane integrity.

RHE tissues were exposed to PM at 0 (Control), 3, 15, or 30 µg/cm² for 24h.

Experiments were repeated at least four times in duplicate.

Results are presented as mean ± SD ; ** $p<0.01$; *** $p<0.0001$ compared to the Control.

A. RHE functionality was assessed 24h after PM-exposure using MTT assay. Results are expressed in absorbance (arbitrary units).

B. Membrane integrity of RHE was evaluated 24h after PM-exposure by intracellular lactate dehydrogenase (LDH) release expressed in arbitrary unit per liter (U/L).

Maximal LDH activity was obtained after 5% SDS treatment (Positive control).

Fig. 3. Inflammatory response of RHE after PM-exposure.

RHE tissues were exposed to PM at 0 (Control), 3, 15, or 30 µg/cm² for 24h.

After exposure cytokine secretions [IL-1α (plain bar) and IL-8 (dashed bar)] were measured by immuno-quantification (ELISA test) in the culture medium in the basolateral compartment.

Data are representative of 4 experiments repeated in duplicate.

Results are presented as mean ± SD ; *** $p<0.0001$ compared to the Control.

Fig. 4. Changes in 4-HNE expression level after PM-exposure.

RHE tissues were exposed to PM at 0 (Control) or 30 µg/cm² for 24h.

(A) After PM-exposure RHEs were fixed in 4% paraformaldehyde, embedded on paraffin and sliced.

Cross-sections (4 µm) were blocked in BSA/PBS buffer and stained using 4-HNE (protein produced when lipid peroxidation is) and DAPI (nucleus).

Scale bar represents 25 µm ; 200x magnification. Representative pictures of n=3 independent experiments.

(B) Quantification of 4-HNE in comparison to Control using Visilog software version 7.0.

Data are representative of 3 independent experiments. Results are presented as mean ± SD ; *** $p<0.0001$ compared to the Control.

(C) After exposure, total RNA was extracted from tissues using the RNeasy® miniKit and reverse transcribed using the Transcriptor Universal cDNA Master. The gene expressions were normalized with GAPDH housekeeping gene.

Results were obtained by calculating the fold change (FC) between two conditions: exposed *versus* Control. Increased oxidant gene expression was observed: $FC \geq 1.5$.

Results are the mean from one RT-qPCR experiments assessed in duplicate.

Fig. 5. Impact of PM exposure on MMP matrix metalloproteinase.

After PM-exposure of RHEs (30 µg/cm^2), metalloproteinase secretion [MMP-1 (plain bar) and MMP-3 (dashed bar)] were measured by immuno-quantification (Luminex® technology) in the culture medium in the basolateral compartment.

Data are representative of 2 experiments repeated in triplicate.

Results are presented as mean ± SD ; *** p<0.0001 compared to the Control.

Fig. 6. Changes in loricrin expression level after PM exposure.

RHE tissues were exposed to PM at 0 (Control) or 30 µg/cm² for 24h.

(A) After PM-exposure RHEs were fixed in 4% paraformaldehyde and embedded on paraffin. Cross-section of RHE (4 µm) stained using loricrin (major protein of differentiated epidermal cells) and DAPI (nucleus).

Scale bar represents 25 µm ; 200x magnification. Representative pictures of n=3 independent experiments.

(B) Quantification of loricrin in comparison to control using Visilog software version 7.0.

Data are representative of 3 independent experiments. Results are presented as mean ± SD ; *** p<0.0001 compared to the Control

Fig. 7. Changes in mRNA expression levels of genes involved in differentiation, cell to cell junction, anchorage and apoptosis after exposure to 30 µg/cm^2 of PM.

RHE tissues were exposed at 30 µg/cm^2 of PM for 24hours. After exposure, total RNA was extracted from tissues using the RNeasy® miniKit and reverse transcribed using the Transcriptor Universal cDNA Master. The gene expressions were normalized with GAPDH or RPL13 housekeeping gene.

Results were obtained by calculating the fold change (FC) between two conditions: exposed *versus* Control).

mRNA expression was considered as increased when FC ≥ 1.5 (dark grey) and decreased when FC ≤ 0.7 (light grey).

Results are the mean from one RT-qPCR experiments assessed in duplicate.

Fig. 8. MoA hypothesis for PM-induced premature skin ageing.

The mode of action (MoA) hypothesis of the airborne pollution on the premature skin ageing process, using the RHE 3D-skin model exposed to fine particles, is subdivided into key events, associative events and modulating factors. The initial key event is the increase of the oxidative stress, associated with the modulation of the inflammatory response, which results in an overexpression of various genes. Associative events include inhibition of the gap junction communication and anchorage.

Table 1. Sum of main metallic elements and organic components of fine particles ($PM_{0.3-2.5}$) from (Cotonou, Benin) (adapted from Cachon et al., 2014).

Chemicals are expressed as mass composition per mass ($\mu g.g^{-1}$) and volume unit (ng/m^3).

Sampling of fine particles was based on continuous collection using high volume samplers (80 m^3/hr).

Supplementary data

Figure S1. Microscopic observation of the homogeneous dispersion of PM prior RHE-exposure.

Scale bar represents 100 µm; 20x magnification.

Representative pictures of n=3 preparations

Table S1. Chemical composition of the fine particles ($PM_{0.3-2.5}$) collected in (Cotonou, Benin) (Cachon et al. 2014).

PM were collected using a high volume cascade impaction air sampler as described by Billet (2007) and the physicochemical characterization was carried out by studying their size distributions, specific surface areas, organic and inorganic chemicals composition and ionic species as described by Cazier (2016). Chemicals are expressed as mass composition per volume unit ($ng.m^{-3}$).

Billet, S. et al., 2007. Ambient particulate matter ($PM_{2.5}$): physicochemical characterization and metabolic activation of the organic fraction in human lung epithelial cells (A549). Environ. Res. 105, 212–23.

Cazier, F. et al., 2016. Characterisation and seasonal variations of particles in the atmosphere of rural, urban and industrial areas: Organic compounds. J. Env Sci. S44, 45-56.

Highlights

- Airborne particles induce skin damages
- Oxidative and inflammatory pathways modulation after skin exposure to PM
- Premature skin ageing after PM exposure

Fig. 1. **Morphological observations of RHEs after PM-exposure.**

RHE tissues were exposed to PM at 0 (Control), 3, 15, or 30 µg/cm² for 24h. After exposure RHEs were fixed in 4% paraformaldehyde and cross-sections (4 µm) were stained with Mayer Haematoxylin and Eosin (H&E) and observed using an inverted light microscope (Leica DM4000B LED).

Scale bar represents 25 µm ; 40x magnification.

Representative pictures of 3 independent experiments.

(A) RHE Control. 1/*Stratum germinativum*; 2/*Stratum spinosum*; 3/*Stratum granulosum*; 4/*Stratum corneum*.

(B) RHE exposed at (B1) 3 µg/cm² ; (B2) 15 µg/cm² ; (B3) 30 µg/cm².

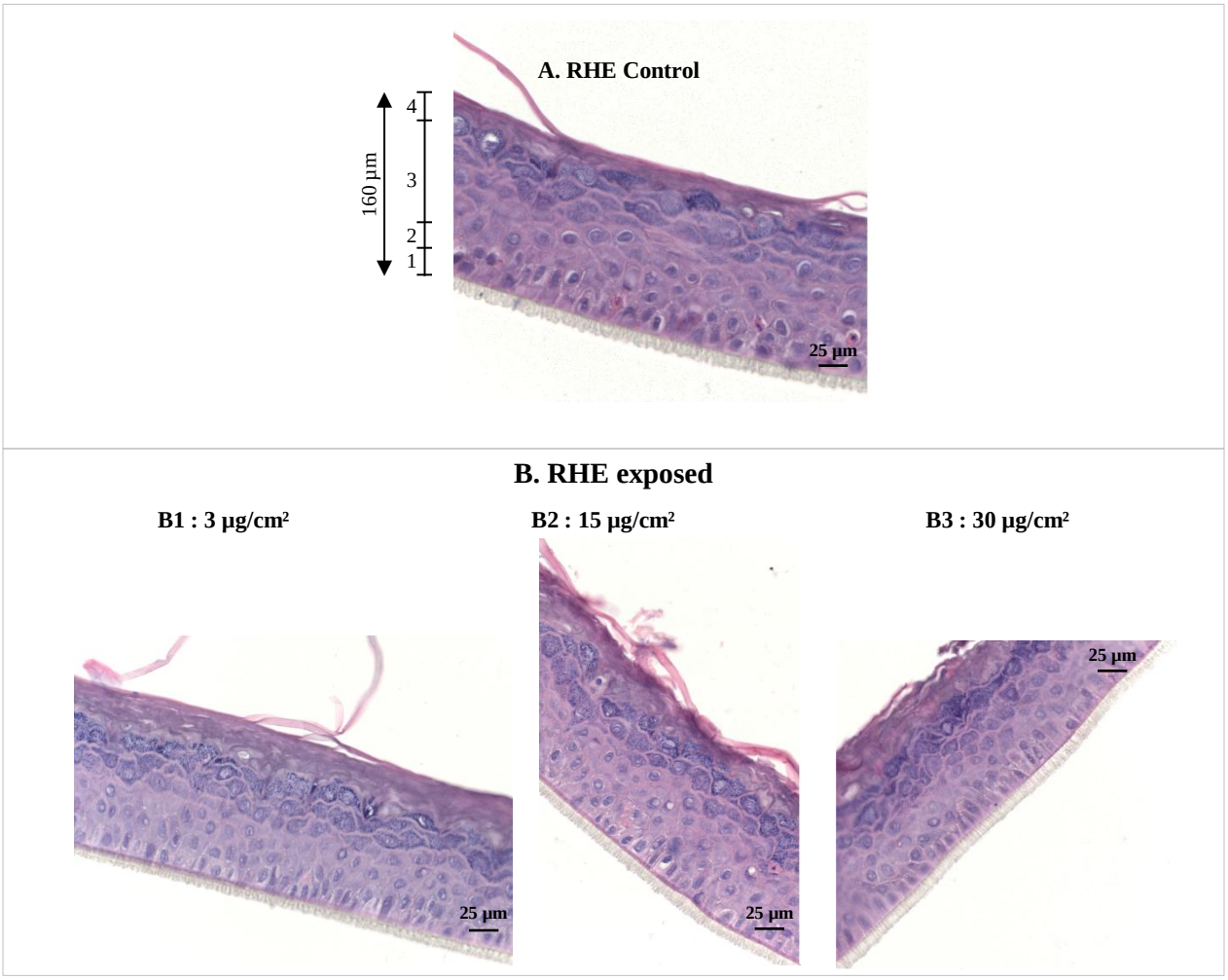

Fig. 2. **Effects of PM on RHE functionality and membrane integrity.**

RHE tissues were exposed to PM at 0 (Control), 3, 15, or 30 µg/cm² for 24h.

Experiments were repeated at least four times in duplicate.

Results are presented as mean ± SD ; ** p<0.01 ; *** p<0.001 compared to the Control

(A) RHE functionality was assessed 24h after PM-exposure using MTT assay. Results are expressed in absorbance (arbitrary units).

(B) Membrane integrity of RHE was evaluated 24h after PM-exposure by intracellular lactate dehydrogenase (LDH) release expressed in arbitrary unit per liter (U/L).

Maximal LDH activity was obtained after 5% SDS treatment (Positive control).

A.

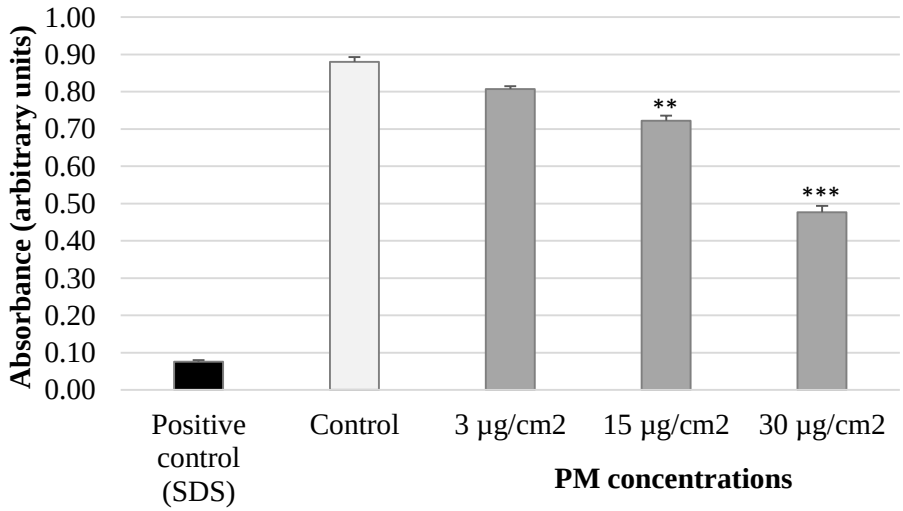

B.

	Positive control (SDS)	Control	3 µg/cm²	15 µg/cm²	30 µg/cm²
LDH release (U/L)	822 ± 31***	15 ± 5	20 ± 10	30 ± 18	41 ± 21

Fig. 3. Inflammatory response of RHE after PM-exposure.

RHE tissues were exposed to PM at 0 (Control), 3, 15, or 30 µg/cm² for 24h.

After exposure cytokine secretions [IL-1α (plain bar) and IL-8 (dashed bar)] were measured by immuno-quantification (ELISA test) in the culture medium in the basolateral compartment.

Data are representative of 4 experiments repeated in duplicate.

Results are presented as mean ± SD ; *** p<0.0001 compared to the Control

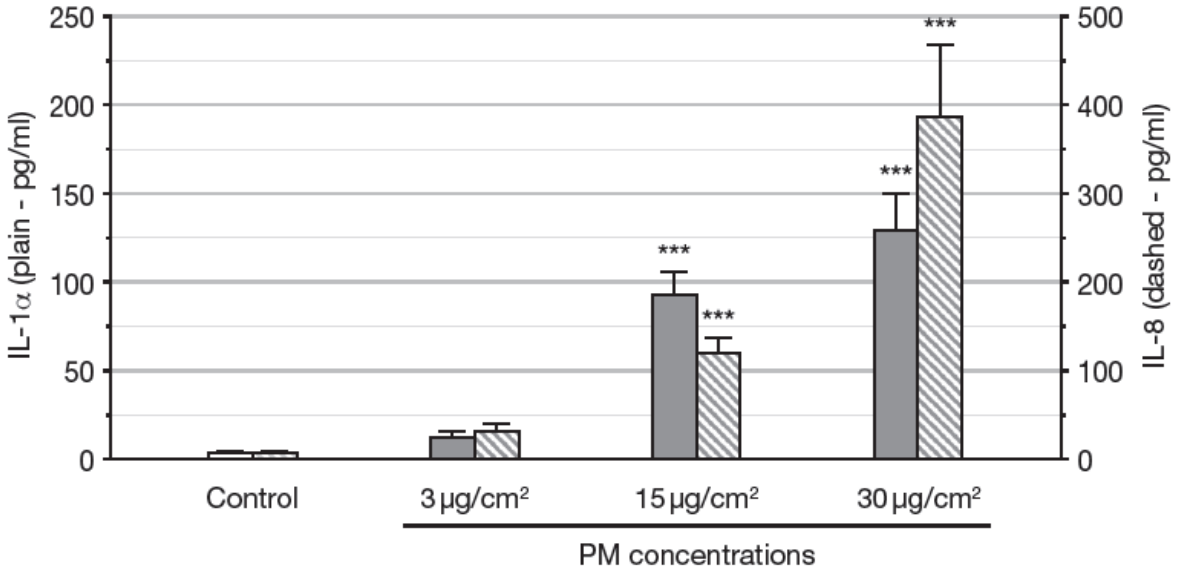

Fig. 4. Changes in 4-HNE expression level after PM-exposure.

RHE tissues were exposed to PM at 0 (Control) or 30 µg/cm² for 24h.

(A) After PM-exposure RHEs were fixed in 4% paraformaldehyde, embedded on paraffin and sliced. Cross-sections (4 µm) were blocked in BSA/PBS buffer and stained using 4-HNE (protein produced when lipid peroxidation is) and DAPI (nucleus).

Scale bar represents 25 µm ; 200x magnification. Representative pictures of 3 independent experiments.

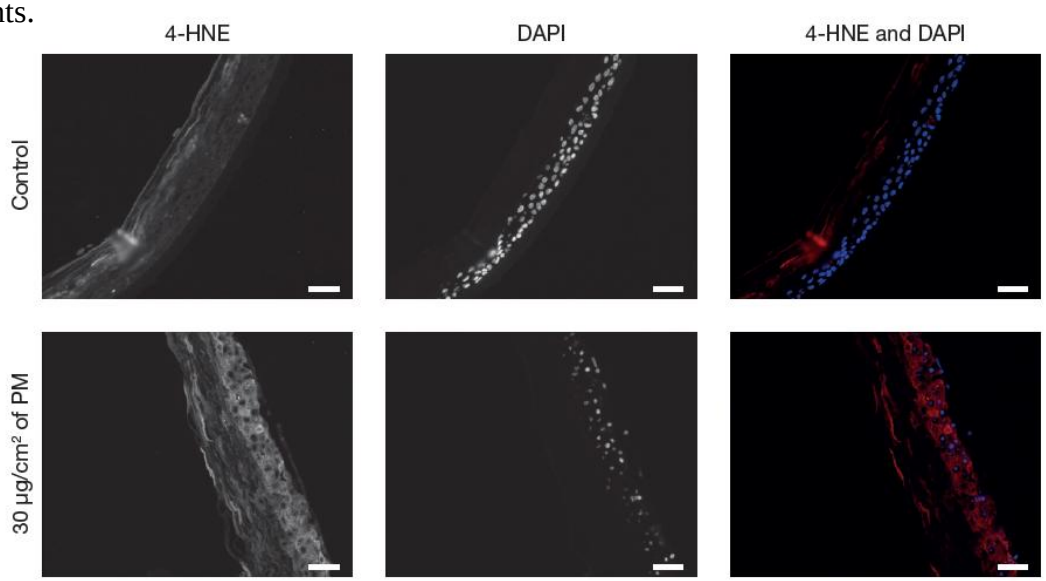

(B) Quantification of 4-HNE in comparison to Control using Visilog software version 7.0.

Data are representative of 3 independent experiments. Results are presented as mean ± SD ; *** p<0.0001 compared to the Control.

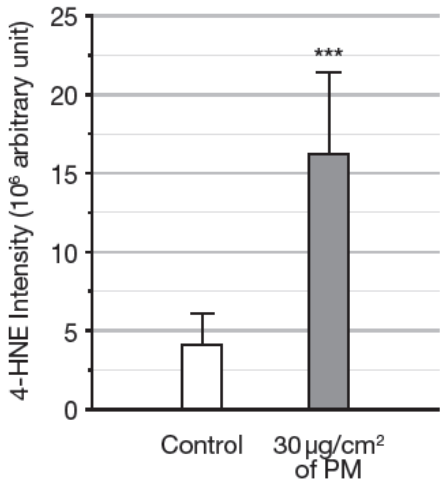

(Fig. 4. continued)

(C) After exposure, total RNA was extracted from tissues using the RNeasy® miniKit and reverse transcribed using the Transcriptor Universal cDNA Master. The gene expressions were normalized with GAPDH housekeeping gene.

Results were obtained by calculating the fold change (FC) between two conditions: exposed *versus* Control.

Increased oxidant gene expression was observed: FC ≥ 1.5.

Results are the mean from one RTqPCR experiments assessed in duplicate.

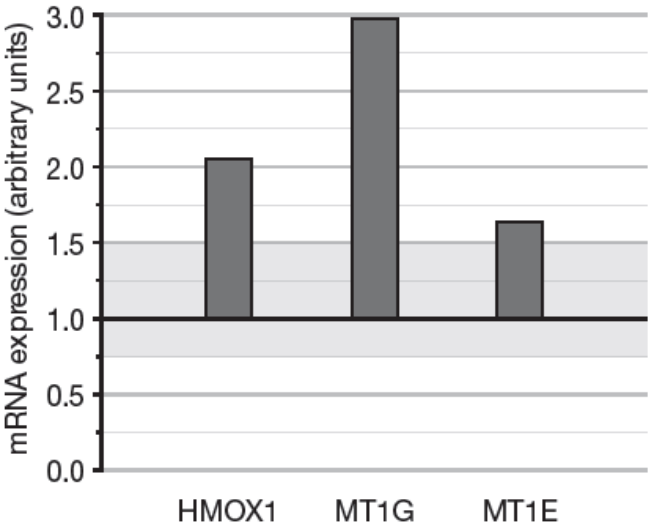

Fig. 5. Impact of PM-exposure on MMP matrix metalloproteinase.

After PM-exposure of RHEs (30 µg/cm^2), metalloproteinase secretion [MMP-1 (plain bar) and MMP-3 (dashed bar)] were measured by immuno-quantification (Luminex® technology) in the culture medium in the basolateral compartment.

Data are representative of 2 experiments repeated in triplicate.

Results are presented as mean ± SD ; *** p<0.001 compared to the Control.

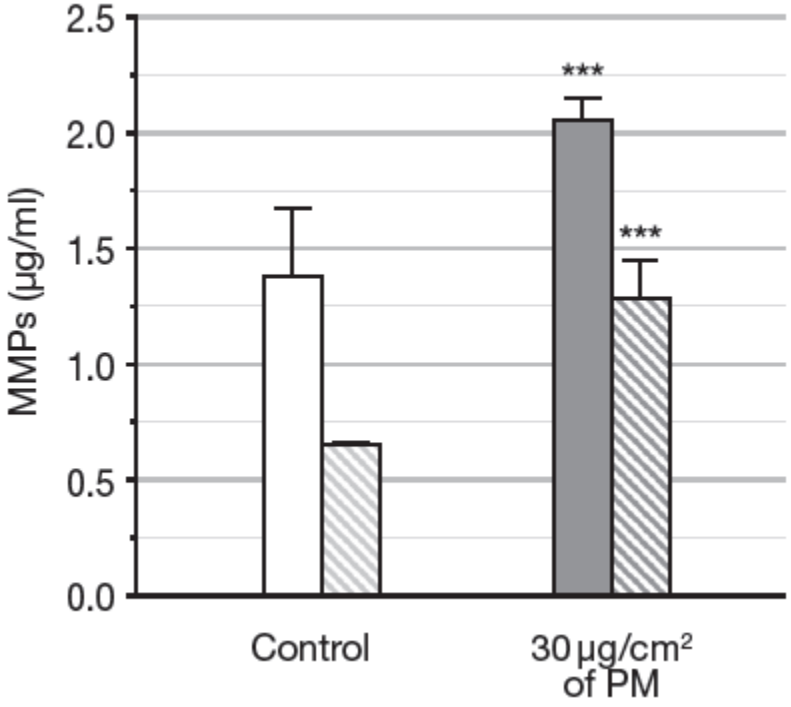

Fig. 6. Changes in loricrin expression level after PM-exposure.

RHE tissues were exposed to PM at 0 (Control) or 30 µg/cm² for 24h.

(A) After PM-exposure RHEs were fixed in 4% paraformaldehyde and embedded on paraffin. Cross-section of RHE (4 µm) stained using loricrin (major protein of differentiated epidermal cells) and DAPI (nucleus).

Scale bar represents 25 µm ; 200x magnification. Representative pictures of 3 independent experiments.

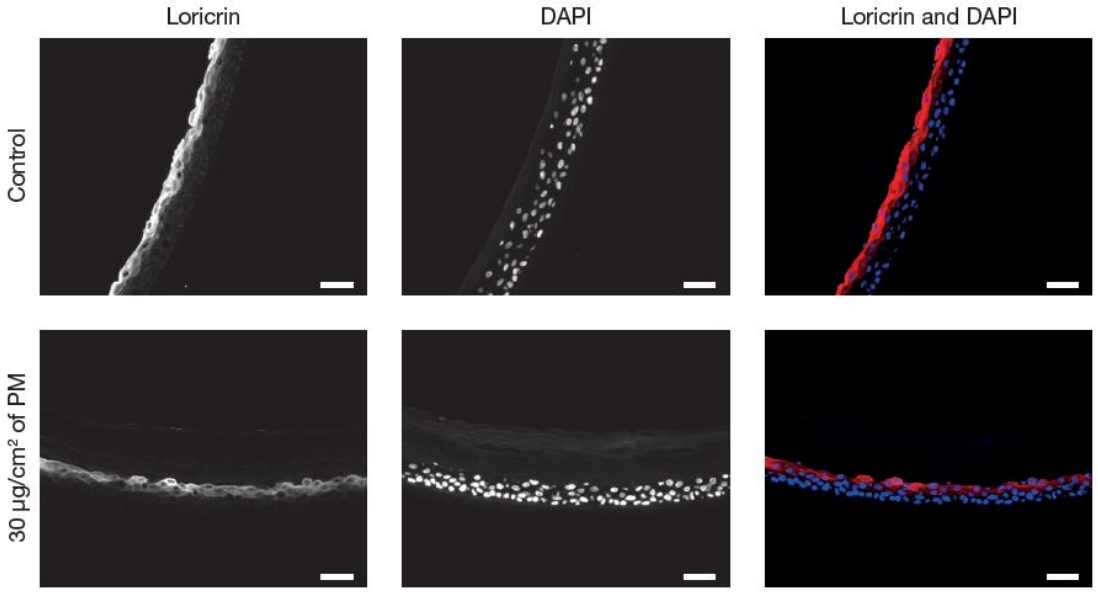

(B) Quantification of loricrin in comparison to control using Visilog software version 7.0.

Data are representative of 3 independent experiments. Results are presented as mean ± SD ; *** p<0.0001 compared to the Control

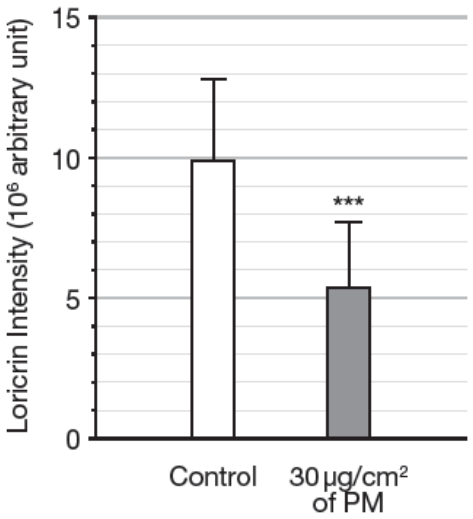

Fig.7. Changes in mRNA expression levels of genes involved in differentiation, cell to cell junction, anchorage and apoptosis after exposure to 30 µg/cm^2 of PM.

RHE tissues were exposed at 30 µg/cm^2 of PM for 24h. After exposure, total RNA was extracted from tissues using the RNeasy® miniKit and reverse transcribed using the Transcriptor Universal cDNA Master. Gene expressions were normalized with GAPDH or RPL13 housekeeping gene.

Results were obtained by calculating the fold change (FC) between two conditions: exposed *versus* Control). mRNA expression was considered as increased when FC ≥ 1.5 (dark grey) and decreased when FC ≤ 0.7 (light grey).

Results are the mean from one RTqPCR experiments assessed in duplicate.

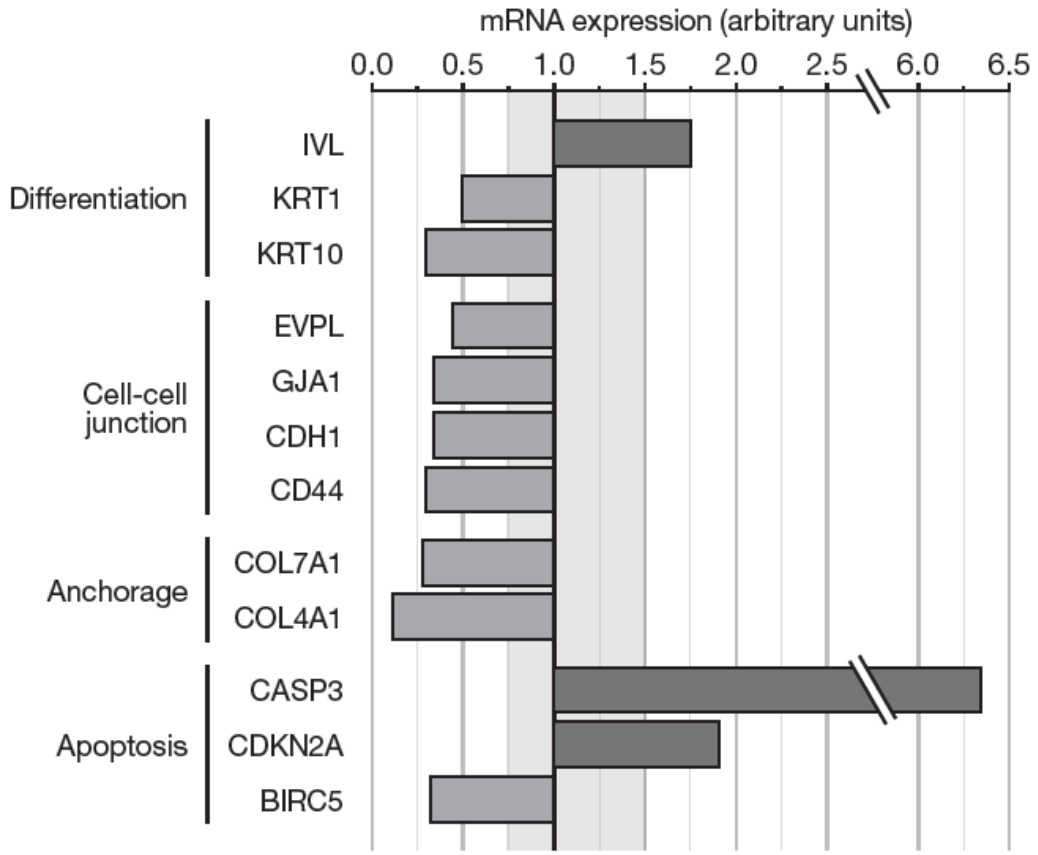

Fig. 8. MoA hypothesis for PM-induced premature skin aging

The mode of action (MoA) hypothesis of airborne pollution on premature skin ageing process, using the RHE 3D-skin model exposed to fine particles, is subdivided into key events, associative events, and modulating factors. The initial key event is the increase in oxidative stress, associated with the modulation of inflammatory response, which results in an overexpression of various genes. Associative events include inhibition of the gap junction communication and anchorage.

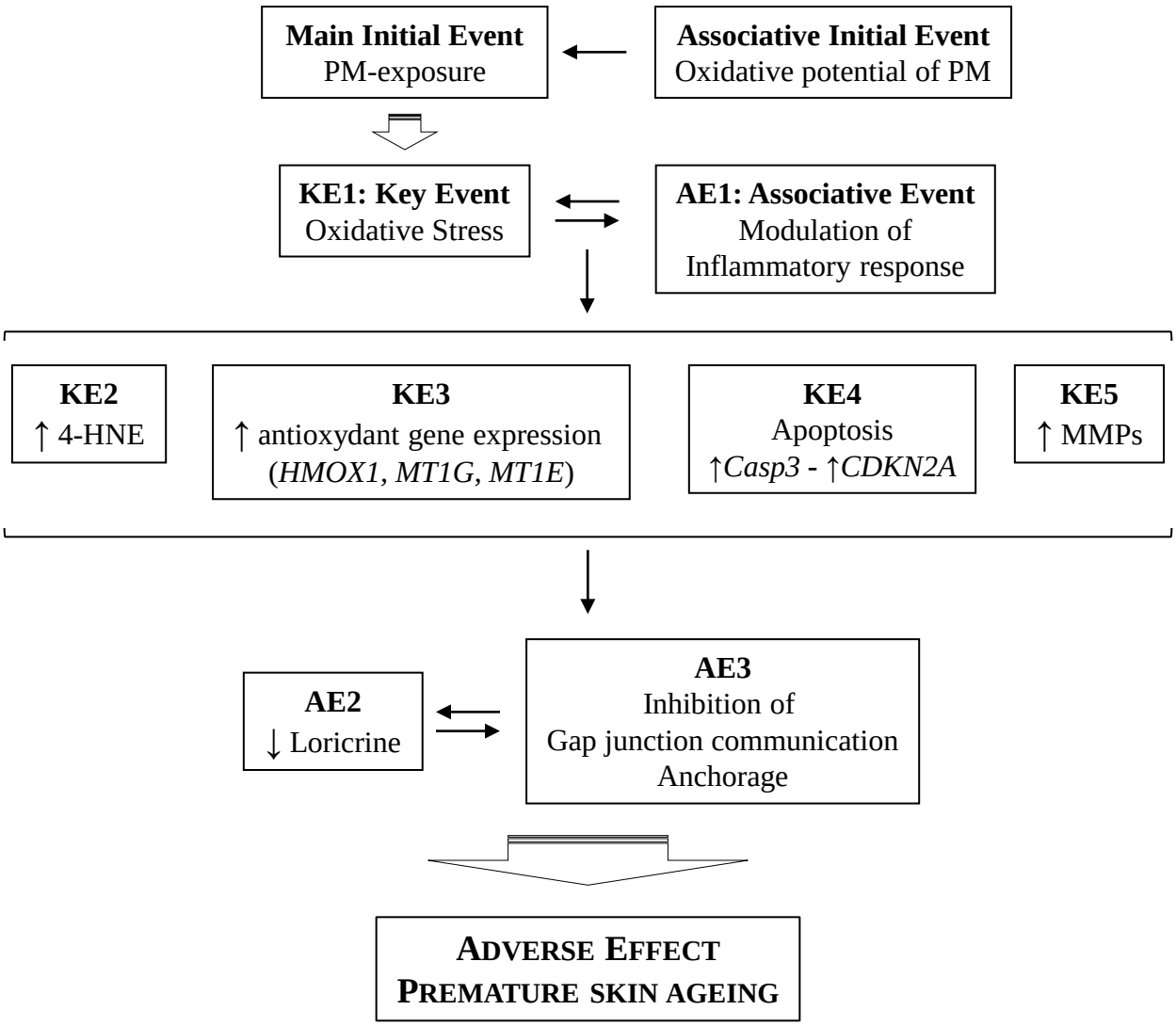

Table 1. Sum of main metallic elements and organic components of fine particles ($PM_{0.3-2.5}$) from (Cotonou, Benin) (adapted from Cachon et al., 2014).

Chemicals are expressed as mass composition per mass ($\mu g.g^{-1}$) and volume unit ($ng.m^{-3}$).

Samplings of fine particles were based on continuous collection using high volume samplers (80 m^3/hr).

	Chemical composition of fine particles $PM_{0.3-2.5}$ Cotonou, Benin, West Africa	
	$\mu g.g^{-1}$	**$ng.m^{-3}$**
Major and trace elements		
Al, Ba, Cr, Cu, Fe, Mn, Ni, Pb, Ti, V, Zn		
Sum of elements	**63,723**	**8,644**
Organic compounds		
Benzene, Toluene, o,p-Xylene, Naphtalene, Phenanthrene, Alkyl-benzene, Benzo[a]pyrene, Benzo[g,h,i] perylene, *etc* …		
Sum of organic compounds	**78**	**11**